Cerebral Cortex December 2009;19:2848–2864
doi:10.1093/cercor/bhp058
Advance Access publication April 9, 2009

Cortical Mechanisms for Online Control of Hand Movement Trajectory: The Role of the Posterior Parietal Cortex

Philippe S. Archambault[1,2], Roberto Caminiti[1] and Alexandra Battaglia-Mayer[1]

[1]Department of Physiology and Pharmacology, SAPIENZA, University of Rome, Italy

[2]Current address: School of Physical and Occupational Therapy, McGill University, Montréal, Canada

The parietal mechanisms for the control of hand movement trajectory were studied by recording cell activity in area 5 of monkeys making direct reaches to visual targets and online corrections of movement trajectory, after change of target location in space. The activity of hand-related cells was fitted with a linear model including hand position, movement direction, and speed. The neural activity modulation mostly led, but also followed, hand movement. When a change of hand trajectory occurred, the pattern of activity associated with the movement to the first target evolved into that typical of the movement to the second one, thus following the corresponding variations of the hand kinematics. The visual signal concerning target location in space did not influence the firing activity associated with the direction of hand movement within the first 150 ms after target presentation. This might be the time necessary for the visuo-motor transformation underlying reaching. We conclude that online control of hand trajectory not only resides in the relationships between neural activity and kinematics, but, under specific circumstances, also on the coexistence of signals about ongoing and future hand movement direction.

Keywords: eye movement, hand movement, online control of hand movement, target jump, posterior parietal cortex

Introduction

An important aspect of motor behavior is the ability to make fast corrections of hand movement trajectory after sudden changes in target location. Given enough time for correction, subjects will not reach the first target, but produce a curved trajectory toward the second one (Carlton 1981; Georgopoulos et al. 1981, 1983; Soechting and Lacquaniti 1983). Movement can also be updated without awareness of target's shift, that is, during saccades (Blouin et al. 1995), when vision of the arm is occluded (Pelisson et al. 1986), and in deafferented patients lacking proprioception in their limbs (Bard et al. 1999; Sarlegna et al. 2006). To perform online corrections, the nervous system might use a nonsensory feedback mechanism based on motor outflow (Desmurget and Grafton 2000), as well as sensory information, such as retinal error (Blouin et al. 1995; Desmurget et al. 1999).

Several studies support a role of the posterior parietal cortex (PPC) in the online control of movement. PPC neurons display activity related to eye and hand position and movement direction, as well as to the location of visual targets in space (for reviews see Andersen and Buneo 2002; Battaglia-Mayer et al. 2003). They also combine different directional eye and hand signals in a spatially congruent fashion (Battaglia-Mayer et al. 2000, 2001). Parietal cortex, dorsal premotor and motor cortex (Johnson et al. 1996; Battaglia-Mayer et al. 2001) form a recurrent network (Marconi et al. 2001) that might be involved in the planning, execution and control of reaching to visual targets.

In humans, perturbation of PPC activity by unilateral transcranial magnetic stimulation (TMS) disrupts the ability to correct hand movements in response to a change in target location (Desmurget et al. 1999; Johnson and Haggard 2005), and prevents adaptation to a new dynamics when movement is made in a velocity-dependent force field (Della-Maggiore et al. 2004). Lesions of the PPC in humans often lead to optic ataxia (OA), an impairment of visual control of arm movements (see Battaglia-Mayer and Caminiti 2002; Battaglia-Mayer et al. 2006, and the references therein) characterized, among other deficits, by a difficulty to produce smooth corrections of hand trajectories following a rapid change of target location (Pisella et al. 2000; Grea et al. 2002). This result, however, has been obtained in a single patient with a large bilateral occipito-parietal lesion and needs to be replicated.

In the cerebral cortex, so far the neural activity during online movement corrections has been investigated only in one study devoted to single-cell analysis in the primary motor cortex (MI) (Georgopoulos et al. 1983). In this study it was shown that MI cells carry signals about the updating of hand movement direction to visual targets. Motor cortex is linked to area 5 both directly (Strick and Kim 1978; Johnson et al. 1996) and indirectly, through dorsal premotor cortex (Johnson et al. 1996; Matelli et al. 1998). Transient inactivation of premotor cortex with TMS results in a reduction of visually dependent online corrections of reaching during sensorimotor adaptation (Lee and van Donkelaar 2006). Therefore, it is reasonable to assume that the information used by motor cortical cells to update hand movement trajectory originates, at least in part, in the superior parietal lobule (SPL). The objective of the present study concerns the role of the SPL in the online correction of hand movement trajectory, both at the level of single cells and of the neuronal population. To this aim, cell activity was recorded in area 5 while monkeys make reaches to visual targets as well as online corrections of movement trajectory, prompted by a sudden change of target location.

Methods

Animals and Tasks

Two male rhesus monkeys (*Macaca mulatta*; body weights 5.2 and 6.0 kg) were used in the study, in accordance with the guidelines of the Italian national law (D.L. 116/92). The animals sat in a primate chair with their head and the unused arm fixed. All tasks were performed in total darkness. To avoid dark adaptation, during the intertrial interval (ITI, 1 s) the room light was turned on.

Reaching Tasks

Monkeys performed arm reaches to visual targets in 3-dimensional space under 2 different intermingled conditions. They used the arm contralateral to the hemisphere of recording.

1. *Single-step task (SST)*. Animals performed hand movements from a central push-button to 1 of 8 peripheral visual targets, arranged at the vertices of an 8.5 cm radius virtual cube (Fig. 1*A*). The central button was mounted on a retractable rod, 17.5 cm from the animal's midline and at shoulder level, while the peripheral targets were presented by 2 robot arms. The sequence of the SST (Fig. 2*A*) was as follows. First, the central button was turned on green to indicate the beginning of the trial. The animal was required to press and fixate this button for a variable control time (800–1500 ms; CT). During this time, the robot arms moved the target into the position required for the subsequent hand movement. At the end of the CT, one of the robot arm buttons was turned green while the central button was turned off. The monkey was required to quickly reach and then press the peripheral target for a variable time (500–1000 ms; target holding time, THT). The rod supporting the central button was mechanically retracted out of the workspace immediately after the release of the button, so as not to impede the subsequent hand movement. The monkey was allowed to freely move its eyes after the initial central fixation period.

2. *Double-step task (DST)*. In 50% of the reaching trials, the peripheral target changed position, either during the reaction time (RT) (DST_{RT}, 160 ms after the presentation of the first target, Fig. 2*B*) or immediately after the onset of hand movement (DST_{MT}, Fig. 2*C*). This double-step condition was accomplished simply by switching off the first target light (on one robot) and by lighting the other one (on the second robot) at appropriate times. Because both robots were already moved to the appropriate positions during the CT, the target appeared to the monkey to "jump" (Fig. 1*A*) from its original position either to the opposite vertex of the cube (at 180°), or to one adjacent (at 90°) and immediately to the left (for right targets), and vice versa for left targets. Therefore, there were 4 double-step conditions (2 switching times and 2 switching directions). To ensure a one-to-one ratio between the occurrence of single-step and double-step movements, single-step conditions to each of the 8 target directions were presented 4 times as frequently. During a recording session, the monkey performed 5–7 repetitions in each of the DSTs, and 20–28 for each of the SSTs. Single- and double-step trials were pseudorandomized and presented in an intermingled design.

Saccade Tasks

At the completion of the reaching tasks, the monkey performed 2 tasks similar to those described above, but involving eye movements only. These tasks were used as controls, with the goal of identifying the influence of eye-related signals on neural activity recorded in the reaching tasks.

1. *Eye single-step task (ESST)*. The monkey pressed and fixated a central button for a variable CT (800–1500 ms). Then, 1 of 8 peripheral targets was presented at 45° angular intervals on a circle of 18° visual field radius (Fig. 1*B*). The monkey was required to make a saccade to the target, and to fixate it for 500 ms, maintaining the button pressed for the entire duration of the trial.

2. *Eye double-step trials (EDST)*. In 50% of the eye movement trials, the peripheral target was suddenly turned off after its presentation, and replaced by the opposite one at 180° in the circle (Fig. 1*B*). This occurred either during RT (160 ms after the presentation of the first peripheral target) or at the onset of eye movement. During the whole trial, the monkey was required to constantly press the central button. Double-step trials were repeated 4–5 times each and single-step conditions 8–10 times.

Behavioral Control

The switching of lights and the movement of the robots were controlled using custom-made software that also recorded the time of the button press and its release. Eye position signals (vertical and horizontal angles) were recorded by using an implanted scleral search coil (1° resolution) sampled at 200 Hz (Remmel Labs, Ashland, MA). Fixation accuracy was controlled through circular windows (5° diameter) around the targets. Arm position was recorded in 3 dimensions using an opto-electronic system (Optotrak, Northern Digital, Waterloo, Canada) with a sampling frequency of 100 Hz. Six markers were attached to a tight-fitting sleeve, which was placed on the monkey's forearm. Hand trajectories were reconstructed offline (see below).

During the reaching task, an upper limit was placed on the hand RT, to make sure that the monkey moved as fast as possible after the presentation of the peripheral target. This limit was set as the mean RT plus one standard deviation of all the trials recorded during the last 2 weeks of training. Because the RT varied between monkeys and for the different target locations, the time limit was set accordingly and ranged from 285 to 335 ms. Hand movement time (MT) was also limited to 350 and 600 ms for single-step and double-step trials, respectively. For the latter, we permitted a longer MT to let the monkeys free to choose

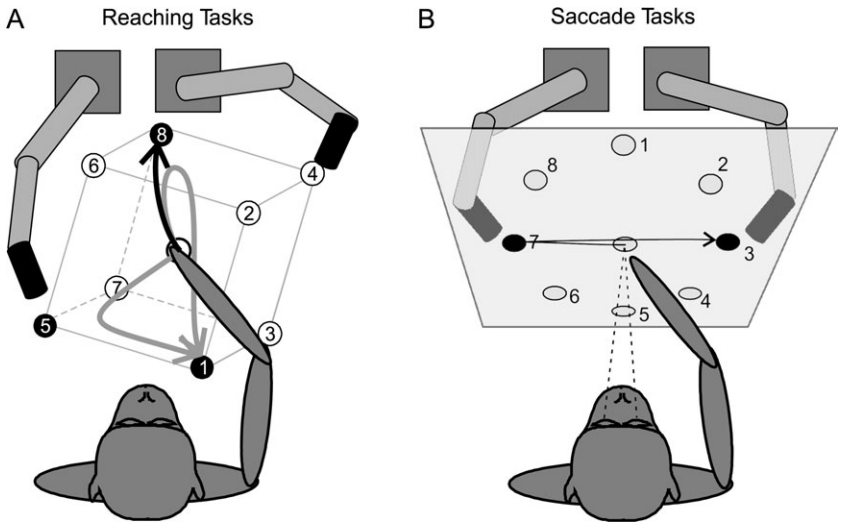

Figure 1. Apparatus and tasks. (*A*) Monkeys performed the reaching tasks (SST, dark arrow and DST, gray arrow) by making hand movements from a central position to peripheral targets arranged at the vertices of an imaginary cube. At the center, a lit button located at the top of a retractable rod was used as the hand starting position. Lit targets were placed behind transparent push-buttons moved by 2 robot arms. In the DST trials the second target could appear either at 180° (opposite) or at 90° (adjacent) with respect to the first target. The peripheral targets of the 3 represented movements are shown in black. (*B*) The same apparatus was used for the SST and DST conditions in the saccade tasks. In this example the final target "jumps" from position 7 to the opposite one, and the monkey first fixates the central light, then directs its gaze to target 7 and finally to target 3.

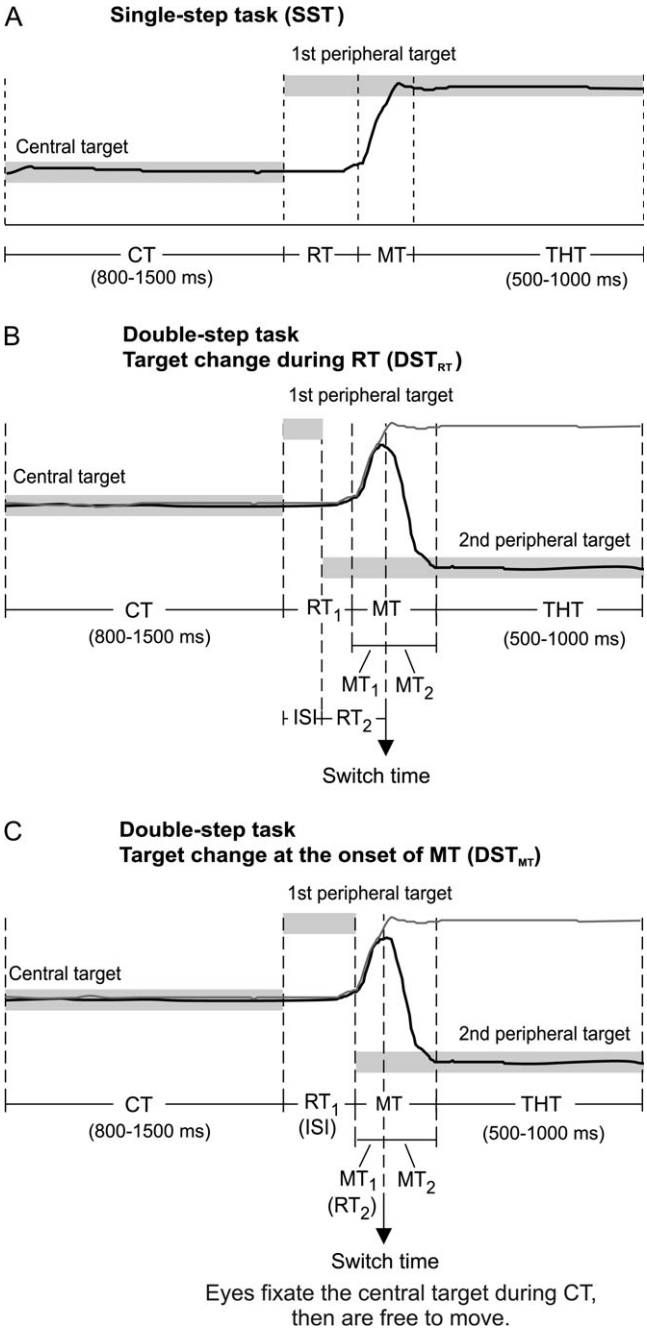

Figure 2. Temporal structure of SST (*A*) and DST (*B*, *C*). In DST, target change occurred during RT (*B*), or at the onset of hand MT (*C*). Gray bars indicate the duration of different visual targets, black lines represent typical time course of hand position in each task. In (*B*) and (*C*), for comparison purposes, hand positions of typical single-step trials are indicated (gray curves). RT_1 and RT_2: hand reaction time to the first and the second target, respectively, in the DST. MT_1 and MT_2: hand MT to the first and the second target, respectively, in the DST. ISI is the time between the presentation of the first and the second target.

their own strategy of movement correction. For the eye task, RT and MT together had to be less than 400 ms. Trials were aborted if these limits were exceeded, then repeated later. Successful trials were rewarded with apple juice.

Neural Recording

The activity of single neurons was recorded with extracellular electrodes, using a 7-channel array (Thomas Recording GmbH, Giessen, Germany). Signals from the electrodes were preamplified, filtered, amplified, and then sent to 7 dual time–amplitude window discriminators (Bak Electronics, Inc., Mt. Airy, MD). This gave the possibility of recording up to 14 cells simultaneously, although generally 5–10 neurons were recorded at the same time. Electrodes were glass-coated tungsten–platinum fibers (1–2 MΩ impedance at 1 kHz). The eye-coil, recording chamber and head-holder were implanted aseptically under general anesthesia.

Data Analysis

The hand kinematics data were used to calculate the time length of the different behavioral epochs (RT, MT, and, importantly, the time of shift of hand trajectories in the DST tasks). Two types of analyses were performed on the neural data. The first type involved the modeling of the neural activity, to examine its relationship with the animal's behavior in both SST and DST conditions. The second type aimed at determining when in time different visuo-motor signals related to the tasks under study emerged in neural activity. In particular, those signals related to the preparation of a hand movement and those related to the updating of the hand trajectory after a sudden target "jump" occurred in different conditions.

Reconstruction of Hand Trajectories

Hand trajectories were reconstructed independently for each recording day, to take into account small variations in the placement of the sleeve on the arm. The relationship between hand position and the markers placed on the monkey's forearm was calculated using a known reference point, that is, when the hand rests on a fixed peripheral target at the end of movement. This operation was then applied to all other data points.

The location and orientation of a rigid body in space is determined by 3 sets of coordinates. In our set-up, we had 6 markers. To increase the accuracy in the calculation of the position of the forearm (and therefore of the hand), we adopted an algorithm based on singular value decomposition, which makes use of the redundant information, in the least-squares sense (Soderkvist and Wedin 1993). The resulting hand trajectories were then smoothed using a 5-point triangular filter.

Behavioral Epochs

The beginning and end of hand movements were taken as the time when the monkey released the central button and pressed the peripheral one, respectively. Additionally, we determined the time of the change in the direction of hand movement during double-step conditions. This was done by first calculating the mean and confidence interval of the hand trajectory in the x, y, z coordinates, over all single-step movements to each of the 8 targets. The 95% confidence interval was obtained using bootstrap statistics. Because the monkeys were well trained, they produced very stereotyped movement trajectories. Therefore, with 20 or more trials available in each of the single-step conditions, the confidence intervals were small. The hand shifting time was then calculated by comparing each double-step trajectory with the mean single-step movement to the same target. The time of hand shifting was defined as the first of a series of 3 points exiting its confidence interval in any of the x, y, or z coordinates.

For the eye, the angular velocity was first derived from the position signals. The onset and offset of the saccade was taken as the first of a sequence of 3 points exceeding or falling below a threshold of 50°/s, respectively. There was no need to calculate a shift time for the double-step conditions, as the eye always completed the saccade to the first target before moving to the second one.

With these values, we could define various epochs describing the animal's behavior (Fig. 2). In the *Reaching* task, the CT ended with the presentation of the first peripheral target. In single-step conditions (Fig. 2*A*), the RT was defined as the time elapsing from the presentation of the target to the onset of hand movement. Only one period of hand movement (MT) was obviously detectable in this task condition. In the double-step conditions (Fig. 2*B,C*), the RT to the second target (RT_2) was calculated from the presentation of the second stimulus to the change in direction of the hand, as determined by the time of hand trajectory shifting (Fig. 2*B,C*). In such cases, the hand MT could be divided in 2 distinct epochs (MT_1 and MT_2), separated by the time of

shift of hand trajectory. MT_1 is the time during which the hand traveled toward the first target, whereas MT_2 is the MT toward the second one. In all cases, the trial finished at the end of THT.

For the single-step conditions of the *Saccade* task, the division into behavioral epochs was the same as in the *Reaching* task (CT, RT, MT, THT). However, because there were 2 distinct movements, in the double-step conditions we defined 2 periods for RT and MT (RT_1 and MT_1 followed by RT_2 and MT_2).

Because saccades were very brief, we also defined the reaction-movement time (RMT) epoch, a combination of RT and MT, to allow one to compare cell activity in the *Reaching* and *Saccade* tasks. In the case of double-step conditions the modulation indices (see below) were computed separately for the 2 different target presentation times and for the 2 submovements ($RMT_1 = RT_1 + MT_1$ and $RMT_2 = RT_2 + MT_2$, see Fig. 2).

Mean Spike Frequency

The mean spike frequency was computed for each epoch and trial. For each task, the modulation of neural activity was assessed using a 2-way ANOVA (factor 1: epoch, factor 2: target position). A cell was defined as being modulated in a given epoch if factor 1 or the interaction term was significant ($P < 0.05$).

Cell Classification

To classify cells as hand or eye related, we compared the modulation of their activity across tasks (reaching and saccade tasks) and movement conditions (single- and double-step). The overall goal was to exclude cells that were equally modulated in the *Reaching* tasks, consisting of both hand and eye movements, and in the *Saccade* tasks, consisting of eye movements only. Indeed, it can be assumed that for such cells the activity observed in the *Reaching* task can also be influenced by eye movements. The classification was based on the use of modulation indices obtained across different tasks and epochs, as well as on bootstrapping procedures. Full details for the methods used are provided in the Supplementary materials.

Modeling of Neural Data

We modeled the neural data using 2 different procedures. The first was a linear regression of each cell's activity, with a time delay, against the position, speed and direction of hand movement. The aim was to explain each cell's activity in the SST and DST tasks using the hand kinematics, and to determine the delay between neural activity and hand movement. The second analysis aimed at modeling each cell's activity in DST using the activity recorded during SST. Although this second analysis also attempted to explain neural activity from behavior, it made no assumption on the exact relationship between activity and hand kinematics.

Linear regression of cell activity. We performed a linear regression of each cell's activity recorded during MT of the reaching task with the corresponding hand kinematics. For the cell activity we computed a spike-density function (SDF). Each spike was replaced by a Gaussian probability function with total area of 1 ms and width (standard deviation) of 30 ms. The SDF was sampled at 100 Hz (the same frequency as for the kinematics) to obtain a continuous function with one value every 10 ms. We processed these data further by subtracting the mean firing frequency during CT (measured over all trials and conditions), and then applying a square-root transform, to make the variance of the SDF independent of its mean (Moran and Schwartz 1999). Both the SDF and the kinematics data were averaged over all trials, independently for each of the SST and DST conditions. The following linear regression model was used:

$$\mathrm{SDF}(t+\Delta t)=\beta_0+\vec{\beta}_1\vec{X}(t)+\beta_2 V(t)+\vec{\beta}_3\vec{D}(t)+\vec{\beta}_4 V(t)\vec{D}(t) \qquad (1)$$

where SDF represents the SDF, $X(t)$ is the hand position vector, $V(t)$ is the speed (magnitude of velocity vector), $D(t)$ is the instantaneous hand direction vector, Δt is the time lag. The regression was applied to values of kinematics and SDF obtained for each 10-ms bin (for a total of ~3400 points, see below). The direction of hand movement was defined as 0 when the monkey's hand was not moving, that is, during central or peripheral THT. The last term represents the interaction between direction and speed of hand movement and was added to account for its known relationship with neural activity (Moran and Schwartz 1999). A total of 11 coefficients were used in the regression, including the constant term.

For a time lag $\Delta t = 0$, the time interval for the kinematics and the SDF data included the MT epoch, together with a fixed 300 ms before its onset, and 300 ms after its offset. The mean data of the 8 SST and 32 DST conditions were placed tip to tail, to generate 2 long signals, one for the kinematics and another for the SDF (for each cell the total length of data was ~3400 points = ~85 point/condition × 40 conditions). The regression coefficients and statistics were then computed.

For time lags $\Delta t \neq 0$, the time interval of the kinematics data remained the same as for $\Delta t = 0$ (MT ± 300 ms). The time interval for the SDF data, however, was shifted by an amount equal to Δt with respect to that of the kinematics. This was done within each of the movement conditions, before assembling the data tip to tail, thus avoiding the overlapping of data from different movement conditions in the assembled signals. For each time shift the linear regression coefficients and statistics were calculated, and the shift yielding the highest regression coefficient was selected as the overall delay for that cell, with negative values indicating that the cell's activity led the hand movement. The time window for the regression analysis (MT ± 300 ms) was deliberately chosen to include the complete RT period as well as a large portion of THT. As a consequence, cells that failed to show an observable peak in R^2 value within this window were discounted (e.g., if the maximum occurred at the edge of the time window, at exactly +300 or −300 ms). Only 6 cells were excluded by this process.

Regression analysis using variants of the model in equation (1) were also attempted (see Supplementary Materials), but produced worse results in terms of regression coefficients. Importantly, the cell delays obtained using the different models were very similar, with the mean delay not varying by more than ±10 ms. These variants included only some of the parameters of equation (1) (e.g., only direction and speed). An attempt was also made to replace hand position with a hand error signal, defined as the difference between the current position of the reach target and that of the hand, but in that case as well the resulting regression values were lower than in the original model (see Supplementary Materials).

Prediction of neural activity patterns in the DST. An observation made by Georgopoulos et al (1983) was that cells in the primary motor cortex, in a DST similar to the one presented here, change their activity pattern following a change in target location and the subsequent hand movement. Thus, the cell activity after the shift in hand movement is qualitatively similar to the one observed when the hand makes a single movement from the center to the second target. This observation was used in our study as a basis to perform another regression analysis, in addition to the multiple-linear regression procedure described above. In this analysis, the objective was to predict the neural activity in DST from that observed during the SST conditions.

We first matched the double-peak hand speed profile in DST with the 2 single-peak speed profiles in the corresponding SST conditions. For example, in a DST trial where the monkey had to reach to target 1, then 8, we would use the SST trials to 1 and 8. Taking only the MT kinematics, we placed the 2 SST trials tip to tail and varied the delay between them. The delay yielding the maximum correlation between the 2 combined SST velocity profiles and the DST velocity profile was calculated. We then applied the reverse procedure to the SDFs: the SST SDFs were placed tip to tail with a delay calculated from the hand velocity profiles. The correlation between the resulting curve and the actual SDF in DST was then calculated. This analysis was performed separately for each target in the reaching task.

To further confirm the results obtained, we compared each DST condition with a randomly selected pair of SST movements. For example, a DST movement to targets 2 and then 7 could be matched with SST movements to targets 1 and 8, etc. We then compared the regression coefficients obtained by matching DST spike activity with either the correct or the random SST movements (paired *t*-test).

Finally, to evaluate the degree of similarity of cell activity associated with the 2 submovements in the DST with that associated with the similar movement performed in the SST, a 2-way ANOVA was performed. In this analysis, direction of hand movement and task

condition (DST, SST) were considered as factors. Cells were judged as displaying no difference of neural activity in the 2 task conditions compared if the task-term was not significant ($P < 0.05$).

Change in Cell Activity during DST Conditions

We performed 2 analyses to determine the time of the change in cell activity following the shift in target during DST conditions. The first was based on the temporal evolution of the correlation between the activity measured in DST and SST. The second measured the time of statistical divergence between DST and SST at the population level.

Comparison of cell activity in SST and DST conditions. The similarity of neural activity across different tasks conditions was investigated through a correlation analysis. The aim was to evaluate if and when a potential neural signal associated with the sudden change of hand movement trajectory emerged in the double-step condition. For each task and movement direction, the mean discharge frequency was computed across different repetitions in a particular time bin (50 ms), and then subtracted from the mean discharge frequency obtained across tasks and replications during the CT. The resulting activity, associated with a particular time bin in a particular task condition, was compared with the one obtained in the same time bin, but during a different task. In such a way, for each comparison and time bin, we obtained a scatter plot, where the x, y components of each data point represent the activity in 2 different conditions (e.g., SST vs. DST_{RT}, see Fig. 13A_{1-2}) for that time bin. The total number of points included in each scatter plot was therefore equal to $N \times 8$, where N is the total number of cells included in the analysis, and 8 is the number of directions tested in the experiment. We then obtained 2 scatter plots for each time bin, corresponding to the following data set comparisons:

- SST versus DST_{RT}
- SST versus DST_{MT}

For each scatter plot, a correlation coefficient (R) was derived, and adopted as a measure of the degree of similarity of neural activity across tasks. In a second step, the evolution in time of the correlation coefficients observed in each time bin was analyzed for 800 ms centered on hand movement onset (Fig. 13*B*). The RT epoch was analyzed "backward" from the onset of MT for the preceding 400 ms as well as "forward" from the presentation of the first target for the following 400 ms. The analysis of RT was performed forward and backward in time to minimize the consequences of temporal misalignment between neural activity and behavior at the end of the temporal scanning, due to the variability in the duration of the epochs across trials. The statistical difference between the correlation coefficients resulting from the comparison of the 2 task conditions, was tested, through a Pearson-Filon statistics with $P < 0.01$ (Raghunathan et al. 1996).

Divergence of cell activity between SST and DST conditions. We were interested in measuring at the cell *population* level the time of change of neural activity following the appearance of the second target in DST. To this end, we measured the divergence in the population SDF (pop-SDF) between the SST and DST conditions. The pop-SDF was calculated by replacing each spike with a unit Gaussian with standard deviation of 10 ms, sampled at 100 Hz. The signals were then averaged over all trials for all cells of each monkey. To account for the variations in the activity of individual neurons with respect to the direction of hand movement we realigned each cell's data to its preferred target direction before computing the pop-SDF. The preferred target direction was defined as the one eliciting the maximal mean firing frequency during RT and MT, for the SST conditions; this was computed separately for the reaching and saccade tasks, whereas the antipreferred target was the one diagonally opposite, that commonly elicited the minimal mean firing frequency under the same task conditions.

To determine the time of divergence in the population activity between the SST and DST conditions, we first calculated the 95% confidence interval of the pop-SDF for the SST trials. The first point of a series of 3 in the SDF for the DST trials that exited this zone of confidence was defined as the time of divergence. This was calculated separately for each target in the reaching task.

Results

Behavioral Data

Reaction Times

The length of the RT was studied in the SST and DST conditions for both the hand and the eye. In both the reaching and saccade tasks, the 2 monkeys behaved very similarly, although the hand RT of the first animal was shorter than that of the second one across all target directions. In the SST, average hand RT to the presentation of the visual target was 305 ms (±26, SD) in Monkey 1, and 348 ms (±31, SD) in Monkey 2. In the DST, the RTs to the first target (RT_1) did not differ significantly from those in SST for the same target. This was expected, because the intermingling of conditions prevented the animal from knowing in advance whether it would have to perform a single- or a double-step hand movement. On the contrary, the RTs to the second target (RT_2) were 254 ms (±36, SD) for Monkey 1 and 278 ms (±38, SD) for Monkey 2, when averaged across DST conditions, therefore, significantly shorter by about 50–70 ms than those observed toward the first target (RT_1) of the DST or in the SST ($P < 0.001$; t-test). In the DST, the second target, presented either at 90° or at 180° relative to the first (see Methods), appeared either during RT, or at the onset of hand MT. We have noticed that the length of RT_2 was related to the time of appearance of the second target. In fact, it was significantly shorter (241 in Monkey 1; 272 in Monkey 2) when the time between the presentation of the 2 targets (interstimulus interval, ISI) was longer, that is, when the second target was presented at the onset of hand movement ($P < 0.01$; t-test). When the second target appeared before the MT onset, the RT_2 were 267 ms (±36, SD) for Monkey 1 and 283 ms (±38, SD) for Monkey 2. All these values, however, did not depend on the new location in space of the final target.

In the reaching task the eye RTs toward the first target were significantly ($P < 0.001$) shorter (mean: 208 ± 24 ms in both monkeys) than those of the hand and did not vary across task conditions. The eye RTs to the second target averaged across DST conditions were 217 ms (±19, SD) for Monkey 1 and 199 ms (±20, SD) for Monkey 2.

Movement Times

In the DST conditions, the duration of the movement toward the first target (MT_1) depended on the ISI, and was shorter when the second target was presented during RT_1 (Monkey 1, 129 ms; Monkey 2, 115 ms) than at the onset of movement (Monkey 1, 257 ms; Monkey 2, 272 ms). This was true, regardless of whether the second target was presented at 90° or at 180° relative to the first one. Obviously, there was a natural increase in the global duration of MT when the second target was displayed at far (180°) rather than at near (90°) distances. The SD of the entire duration of MTs (MT_1 + MT_2) was for both monkeys equal to 53 ms.

Trajectories and Speed Profiles

The hand trajectories were very stereotyped and similar in the 2 animals. In the SST, the hand traveled directly to the target describing a slightly curved trajectory in all movement directions. In the DST, the hand always moved toward the first target and then to the second. The length of the hand path to the first target was a function of the ISI, because it was shorter when the second target was presented during RT_1 and longer

when this occurred at onset of hand movement (Fig. 3). On the contrary, in all instances of the DST the eyes completed the saccade to the first target before making another one to the second target (Fig. 3).

In the SST, the hand described a typical bell-shaped velocity profile characterized by a single peak (Fig. 4*A*). In the DST (Fig. 4*A*) the velocity profile displayed 2 peaks. The first one, relative to the movement to the first target, was followed by a deceleration phase necessary to change the direction of hand movement toward the second target, then by an acceleration period at the end of which the hand attained its second speed peak. The shape of the velocity profile for the movement to the first target was similar to the corresponding part of the curve observed in SST (Fig. 4*B*). The general shape of the hand velocity profile also depended on the time of occurrence of the target change. When the second target was presented at the onset of MT, the deceleration following the first velocity peak was longer than the corresponding one observed when the target jumped earlier (i.e., during RT).

Neural Data

The activity of 240 neurons was recorded extracellularly in the SPL of 2 left hemispheres of 2 monkeys while these performed the tasks described above. In both animals, microelectrode penetrations (Fig. 5) were made in a region of the SPL identified as Brodmann area 5 (area PE) on the basis of the histological reconstructions of the microelectrode penetrations relative to gross anatomical landmarks, such as the position of the intraparietal (IPS) and central sulci, the postcentral dimple, as well as on the basis of the depth of recording. In both animals, electrode penetrations were perpendicular to the cortical surface and the extent of recording was usually confined within 2 mm from the top of neural activity. This indicates that the results of this study refer to the flat exposed part of area 5.

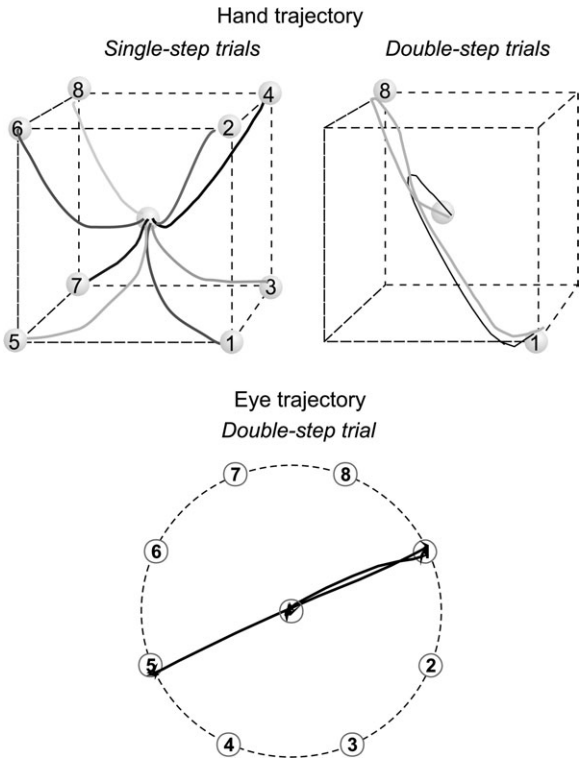

Figure 3. Examples of hand and eye movement trajectories in different tasks (single trials). In SST, hand movement trajectories are shown from their common origin to the 8 different targets located at the vertices of an imaginary cube. In DST, reversal of hand path originally directed to target 8 and then to target 1 is shown after presentation of the second target during RT (black) or at the onset of MT (gray). The eye movement record of the double-step trial of the saccade task refers to the case when target change (from 1 to 5) occurred during the RT. The monkeys always saccade toward the first target and then move their eyes to the second one.

Single-Cell Data

Table 1 displays the proportion of cells that were modulated (ANOVA, $P < 0.05$) during the different epochs of the reaching and saccade tasks on single-step trials. The table also shows the breakdown of this population by monkey. The proportion of hand-related and eye-related cells, selected on the basis of their modulation indices (see Methods) is shown in Table 2. Only the hand-related cells (n = 167/240; 70%) were used for further analysis.

Multiple Regression of Cell Activity

A multiple-linear regression was performed with the aim of studying the relationship between cell activity in area 5 and kinematics parameters, such as hand movement direction, position and speed (eq. 1). All cells displayed a significant relationship between kinematics and activity ($P < 10^{-3}$). It is worth noting that because of the large number of data points in this regression analysis ($n \sim 3500$), an $R^2 = 0.01$ was statistically significant at the 1% level. The results of this analysis are given in Figure 6. It can be seen that cell activity was significantly correlated with hand kinematics. A continuum of values, from weak to stronger ones, characterizes the goodness of the model adopted (Fig. 6*A*). The distribution of the temporal lags yielding the highest regression coefficient of the multiple regression for the population of hand-related cells, averaged across all reaching conditions, is given in Figure 6*B*. It can be seen that the activity of most cells showed a negative delay, indicating that it led hand movement onset, whereas a minority of them had positive delays (median: –20 ms; mode: –75 ms), indicating that neural activity of these cells followed hand movement onset.

The activity of a parietal cell studied in the SST is shown in Figure 7. This cell discharged with natural movements of the contralateral arm toward targets presented at different locations. This cell's activity was modulated in an orderly fashion as a function of the velocity and direction of hand movement. The activity of the same cell in the DST is shown in Figure 8, for all 8 combinations in which the target jumped by 180° at the onset of hand movement toward the first target. In all instances, the pattern of cell activity when the hand moved to the first target changed after presentation of the second one. As in the SST conditions, the cell activity was visibly modulated by hand speed across all the DST conditions tested. For this cell the multiple regression yielded an R^2 of 0.49, and a temporal lag of –80 ms, indicating that the changes in activity led those in motor behavior. Figures 9 and 10 show another parietal cell, whose activity was modulated by hand speed. However, in this case the modulation of neural activity followed the hand kinematics by 90 ms (R^2 = 0.51). We also examined the fit of the model parameters, obtained using all reaching trials, when applied separately to the SST and DST conditions. The same

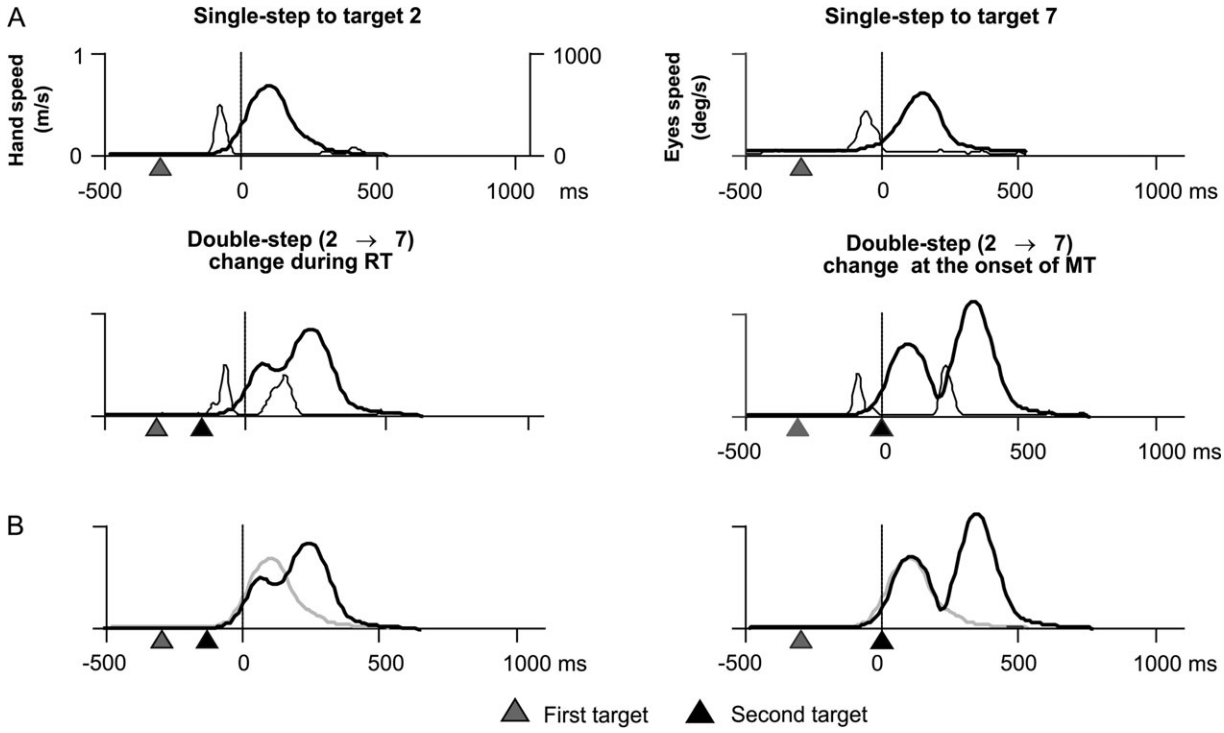

Figure 4. Speed profiles. (*A*) Hand (thick curves) and eye (thin curves) speed profiles for hand movements and saccades in the reaching tasks in 2 different directions of the SST and when changing movement direction from target 2 to target 7, during RT or at the onset of MT in the DST. The gray and black triangles indicate the presentation of the first and the second target, respectively. (*B*) Overlap of hand speed profiles from the SST (gray) for hand movement toward target 2 and DST (black) for target jump (from 2 to 7) during RT (left) or at the onset of hand MT (right).

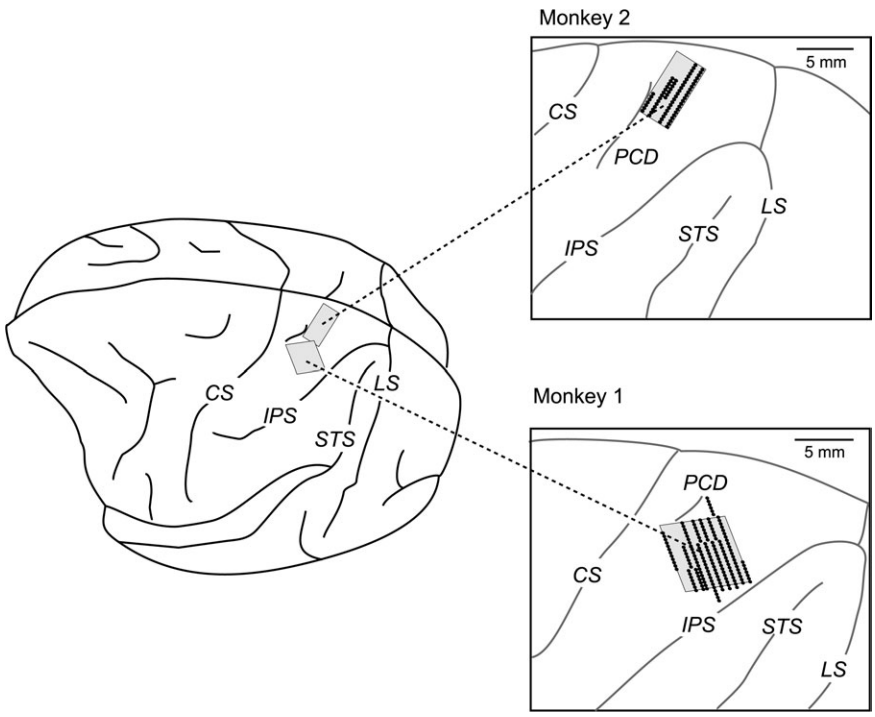

Figure 5. Entry points of microelectrode penetrations in the SPL (Brodmann's area 5). CS, IPS, STS, LS indicate central, intraparietal, superior temporal, and lunate sulci. PCD, postcentral dimple.

parameters were significantly better at explaining cell activity in SST (mean R^2: 0.33) than in the 4 DST conditions (mean R^2: 0.21 – 0.27). An analysis of variance indicated a significant effect of task condition on R^2 values ($P < 0.01$). Post hoc comparisons (Tukey test) confirmed that R^2 values were generally higher in SST, with respect to all the DST conditions.

Predictability of Cell Activity in DST from SST

A behavioral observation which was consistent across monkeys was that the correlation between the DST hand speed profiles and the corresponding SST profiles placed tip to tail (see Methods) was on average high ($r = 0.74$, Pearson). Therefore, an analysis was performed to test whether cell activity during the DST could be predicted from the activity observed in the SST. Figure 11 shows an example of the cell activity predicted in DST, by splicing together the 2 corresponding SDFs in SST, with a delay calculated from matching the speed profiles. For the cell shown, the mean correlation between the predicted and actual SDFs was $r = 0.77$, averaged over all DST conditions. Thus, when the second target appeared in the DST task, the activity of this cell was somehow substituted by that observed when the monkey reached directly to that same target from the initial position, as in the SST task. The distribution of the correlation values between the predicted and actual neural activity profiles, calculated for all cells of both monkeys, is displayed on Figure 11*B*.

Table 1

Modulation (2-way ANOVA, $P < 0.05$) of parietal neural activity in the reaching and saccade tasks

		Reaching—SST						Saccade—ESST			
		CHT versus RT		CHT versus MT		CHT versus THT		CHT versus RMT		CHT versus THT	
	N	Epoch	TxE	Epoch	TxE	Epoch	TxE	Epoch	TxE	Epoch	TxE
Monkey 1	171	68%	31%	90%	67%	79%	56%	47%	6%	49%	9%
Monkey 2	69	90%	26%	100%	25%	36%	0%	16%	0%	20%	4%
Total	240	74%	30%	93%	55%	67%	40%	38%	4%	40%	8%

Note: The percentage of cells refer to those with significant factor 1 (epoch) and interaction factor (epoch × target). In both tasks, only single-step trials were used for this analysis.

Table 2

Functional classes of cells studied in parietal cortex

	N	Hand cells	Eye cells	Eye-hand
Monkey 1	171	64%	25%	11%
Monkey 2	69	84%	6%	10%
Total	240	70%	20%	11%

To validate these results, we repeated the substitution analysis by comparing each DST condition with a randomly selected pair of SST movements. For example, a DST movement to targets 2 then 7 could be matched with SST movements to targets 1 and 8. The regression coefficients obtained when substituting DST with a random choice of pairs of SST movements are presented in Figure 11*C*. These coefficients were significantly lower than those obtained when using the correct SST movements (paired *t*-test, $P < 10^{-6}$).

As a further test, the degree of similarity of cell activity associated with the submovement in the DST with that associated with the same movement in the SST was evaluated by a 2-way ANOVA. Cells displaying no significant ($P > 0.05$) difference of neural activity across these conditions were 92/167 (55.0%).

Results from this analysis, as well as from the multiple-linear regression, show that the neural modulation could be largely explained by the variations of hand kinematics.

Comparison of Cell Activity in SST and DST Conditions

Figure 12 reports a direct comparison of the temporal evolution of the neural activity for the parietal cell shown in Figure 7; data refer to 2 task conditions (SST, gray; DST, black) for 3 different movements. From these examples it is evident the good correspondence of the neural activity around MT onset in the 2 tasks. It is also clear that the time of divergence of the DST activity from the one recorded during the SST (dashed line) occurs before the time of the hand shift, indicated in this figure by the time the 2 velocity profiles start to differ (solid vertical line). Therefore, we addressed the question about the time when a signal related to the updating of hand movement trajectory emerges from neural activity, taking into account the entire population of cells. To this end, we compared by means of a correlation analysis the neural activity of each cell in the SST and DST, for movements oriented initially to the same target. This was aimed at evaluating the similarity of the firings of the cell in the 2 task conditions, for different time bins (50 ms width). For each cell and for each of the 8 possible directions we compared the activities of SST movements toward a given target (e.g., target 8 in Fig. 1*A*), to the activity recorded in DST, when the first target was in the same location and the second in the opposite one

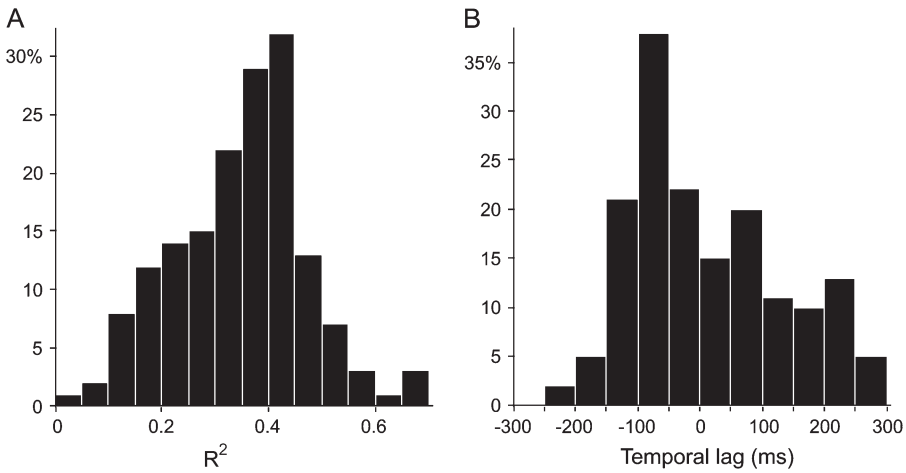

Figure 6. (*A*) Distribution of the R^2 values from the multiple-linear regression analysis. (*B*) Distribution of the temporal lags obtained from the same analysis, for the populations of cells with $R^2 > 0.2$.

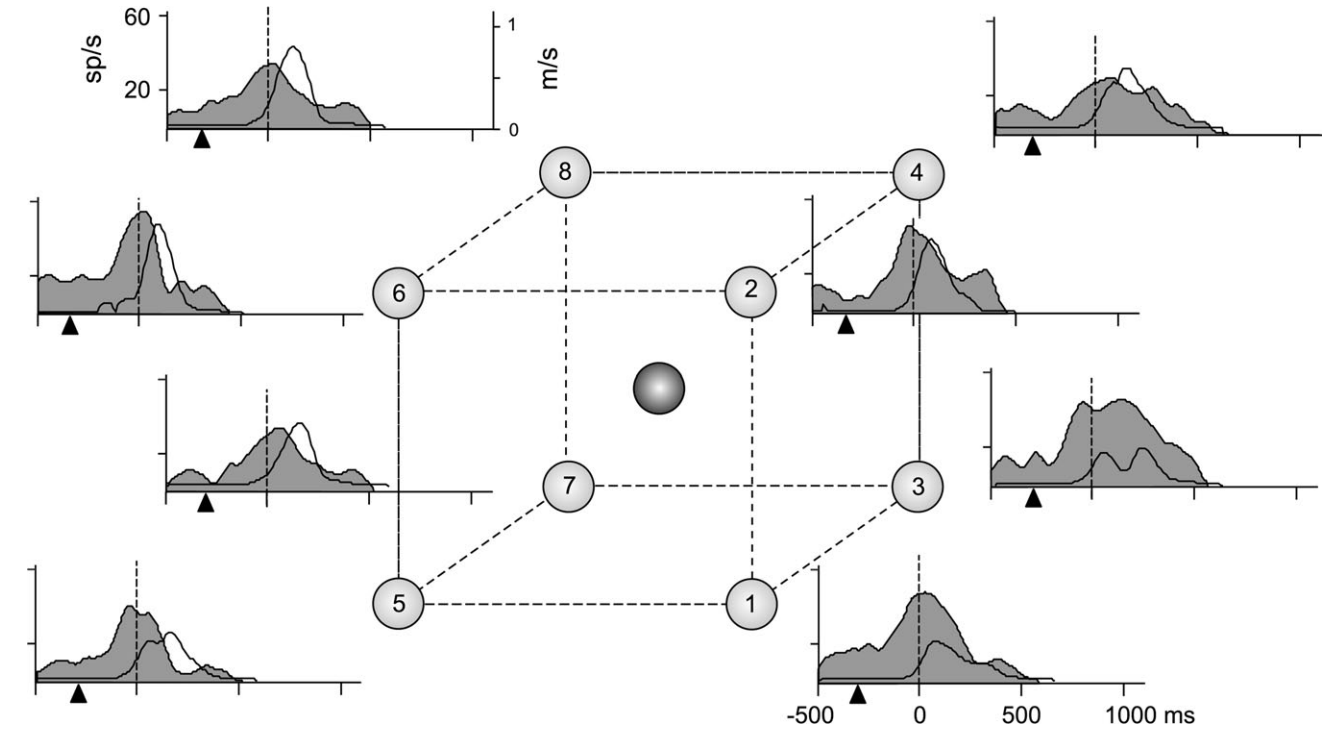

Figure 7. Neural activity of a parietal cell studied during SST. Neural activity is shown in the form of SDF (filled curved) in 8 directions of hand movement. Hand speed profiles recorded during the collection of this cell are shown as black curves temporally aligned to the SDF. On the *x* axis, the triangle shows the mean time of target presentation, the vertical broken line at time zero indicates onset of hand movement.

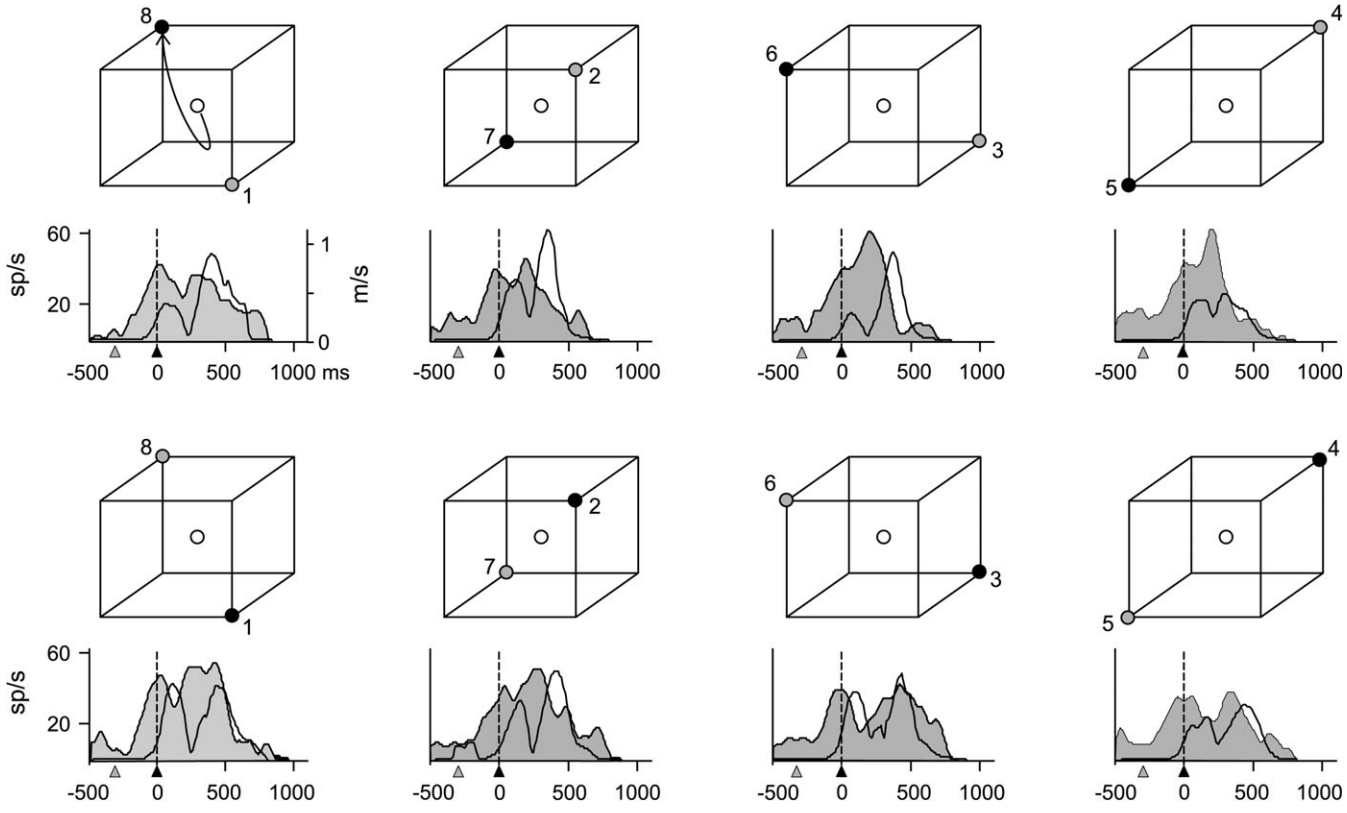

Figure 8. Neural activity in DST_{MT} for the cell displayed in Figure 7. The activity is shown for all 8 combinations in which the second target (black triangles) appeared at 180°, and at the onset of hand movement (vertical broken line at time zero) with respect to the first target (gray triangles). In each cube, the circles represent the location of the first (gray) and the second (black) targets. In the first cube (upper left) a schematic representation of the typical hand trajectory is reported. Conventions and symbols as in Figure 7.

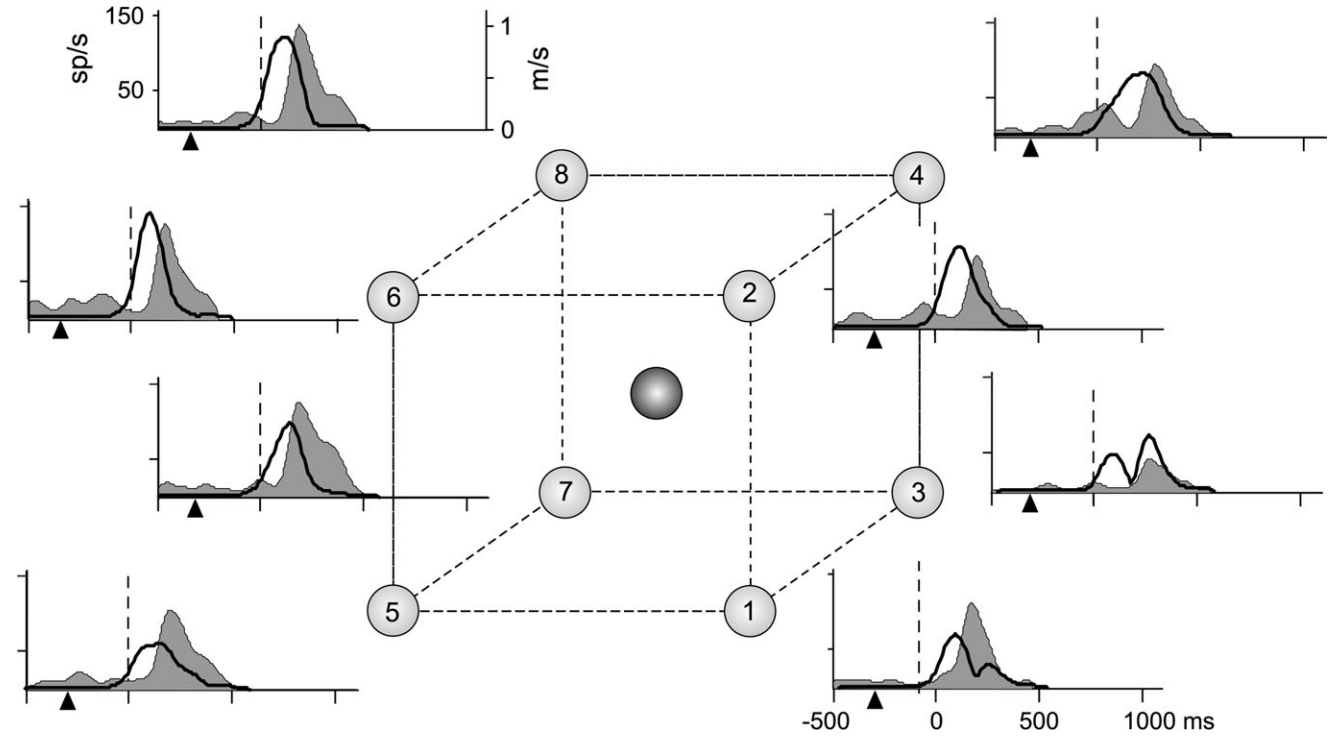

Figure 9. Neural activity of a parietal cell studied during SST, in which the activity follows the hand kinematics. Conventions and symbols as in Figure 7.

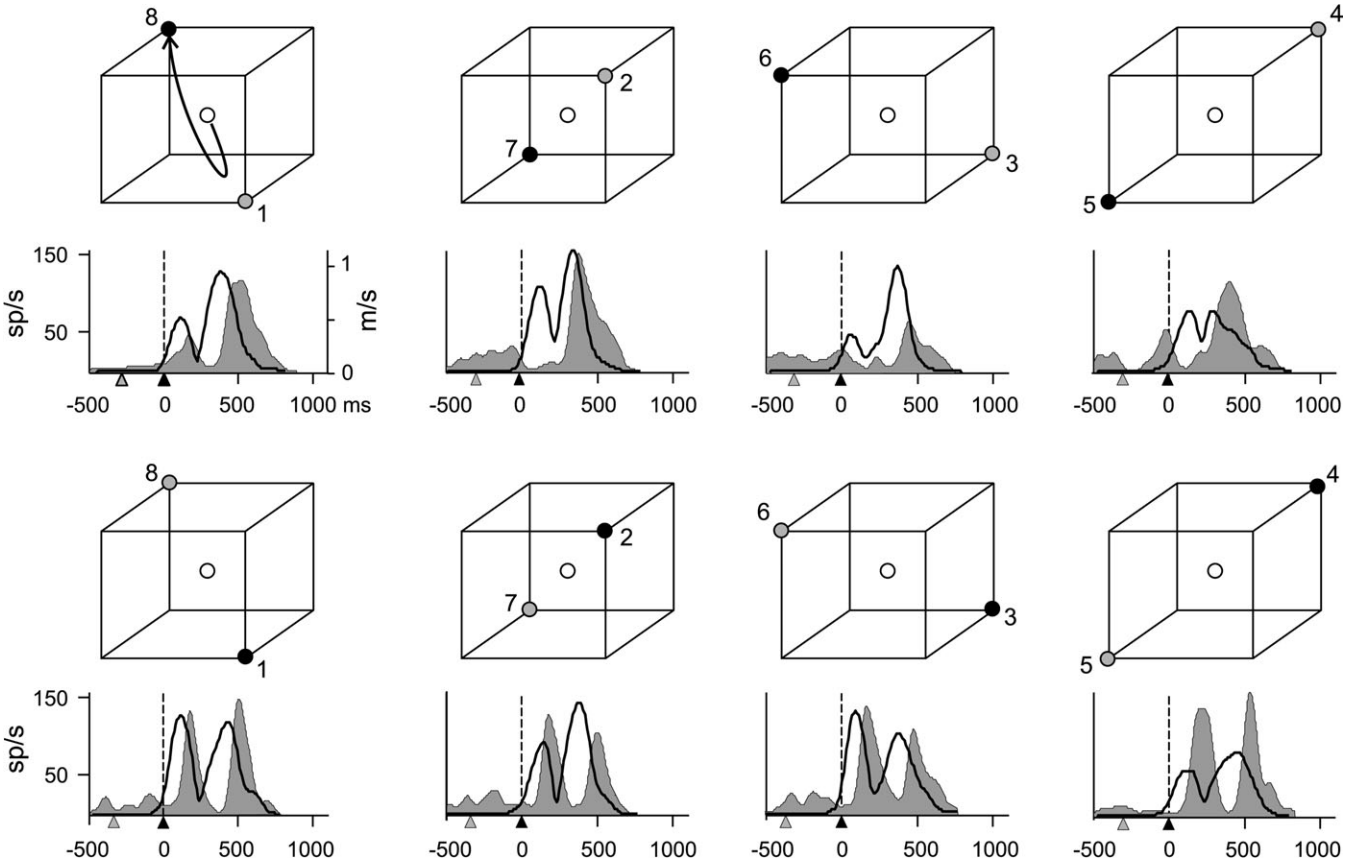

Figure 10. Neural activity in DST_{MT} for the cell displayed in Figure 9. Conventions and symbols as in Figures 7 and 8.

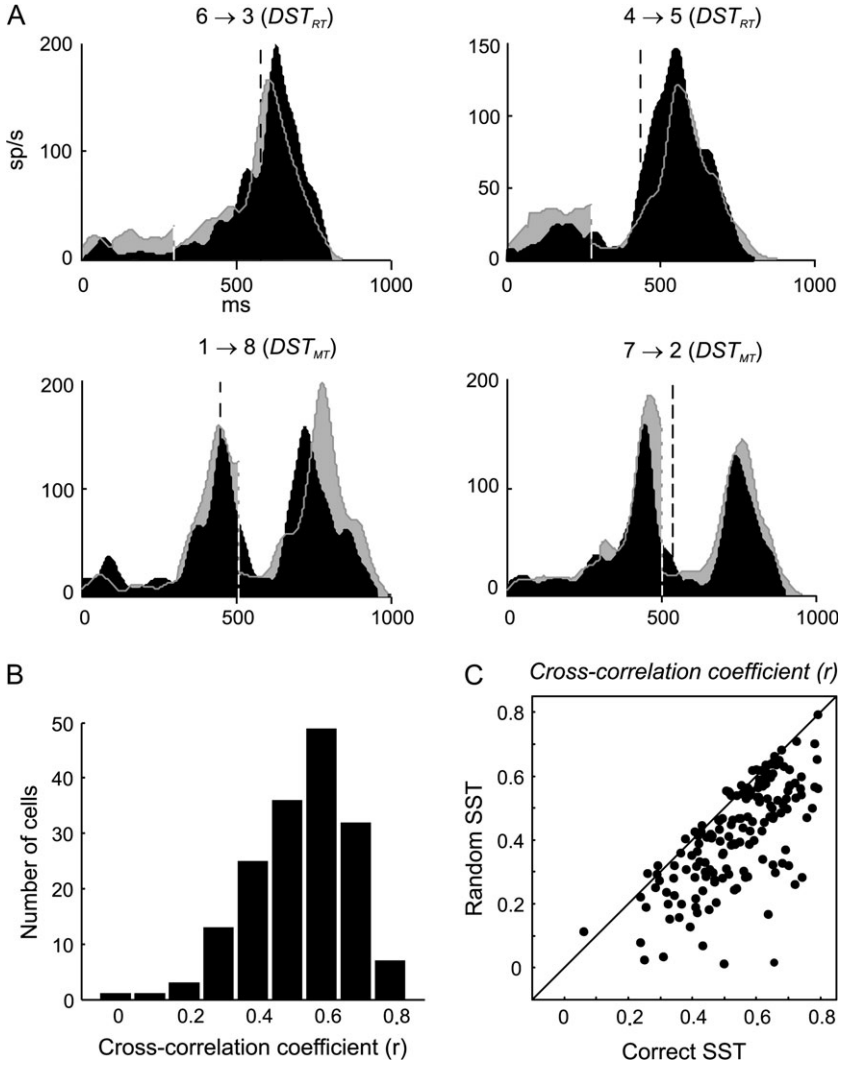

Figure 11. Predicting cell activity in DST from activity in SST. (*A*) Comparison between cell activity observed during DST (black SDF), and that obtained by combining, tip to tail, the 2 SDFs (gray curves) associated with SST trials toward the same targets (see Methods). The figure illustrates data of a single cell in various movement conditions. The numbers indicate the target sequence. DST_{RT} and DST_{MT} indicate that the targets were switched during hand reaction- or at the onset of MT, respectively. The vertical dashed lines represents the time of shift of hand trajectory (black), and the instant of change of cell activity (white) for the first SST movement. (*B*) Distribution of the correlation coefficients between the activity experimentally observed in DST and the one obtained by combining the activity from SST for all cells studied in both monkeys. (*C*) Comparison of the correlation coefficients obtained after matching neural activity from each DST condition with those associated with a randomly selected pair of SST movements (Random SST) or to the corresponding pairs of movement directions of the SST (Correct SST).

(e.g., 8 → 1 in Fig. 1*A*). In this way we studied the time course of the overall correlation of cell firings in different task conditions (SST vs. DST_{RT}, SST vs. DST_{MT}).

The results (Fig. 13) from both monkeys were very similar, and therefore were pooled together. The correlation coefficients were computed from 400 ms before to 400 ms after the onset of MT (Fig. 13*B*,*C*), used as alignment time.

The top row of Figure 13 illustrates 4 examples of cell activity correlation plots obtained at different points in time and for different task comparisons. When comparing SST versus DST_{RT} the cell firing frequencies where initially poorly correlated (Fig. 13A_1), but the correlation was high near the onset of hand MT (Fig. 13A_2). The temporal evolution in correlation between cell firing frequencies indicates that the correlation remained low for approximately 150 ms following the presentation of the first target. Then, it significantly increased ($P < 0.01$, Pearson–Filon statistics), attaining a value of R ~0.8 during the 100 ms prior to MT onset (Fig. 13*B*, left panel). The correlation of firing frequencies declined significantly ($P < 0.01$, Pearson–Filon statistics) 50 ms after the MT onset, that is at approximately 100 ms before the time of shift in hand trajectory for the DST_{RT} (thick vertical line).

The comparison between SST and DST_{MT} yielded similar results (Fig. 13A_{3-4} and 13*B*, right panel). Before MT, the correlation coefficient evolved in the same fashion as for the SST versus DST_{RT} comparison. However, it remained at a high level (R ~0.8) for the 150 ms following the MT onset, that is, until approximately 100 ms before the hand shift time of DST_{MT}.

In both comparisons the correlation was low in the first part of RT, despite the similarity of the tasks compared at this stage (Fig. 13*C*). Furthermore, it is worthwhile to note the behavioral state of the different task conditions, at the time the peaks in correlation between cell firing frequencies (Fig. 13*C*) occurred. In SST versus DST_{RT}, the correlation peaked during the last

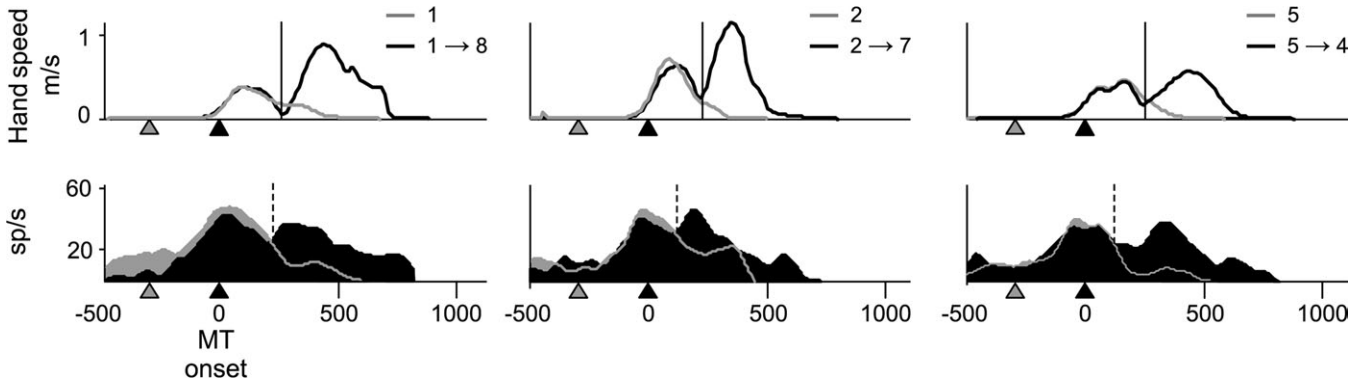

Figure 12. Comparison of hand speed (top) and neural activity (SDF, bottom) for one parietal cell in 2 different reaching tasks (DST_{MT}, black; SST; gray). The 3 panels refer to different movement directions, that is, SST directed to target 1 compared with DST_{MT} directed first to target 1 and then to target 8 (left), SST toward target 2 compared with DST_{MT} directed first to target 2 and then target 7 (center), SST toward target 5 compared with DST_{MT} directed first to target 5 and then target 4 (right). For the locations of the different targets see Fig. 1. The activity is aligned to the MT onset (0 ms), that in this case (DST_{MT}) coincides with the appearance of the second target. The gray and the black triangles refer to the time of the presentation of the visual targets. The vertical lines refers to the time of shift in hand trajectory (solid line) and to the instant the neural activity relative to DST diverges from that recorded during SST (dashed line).

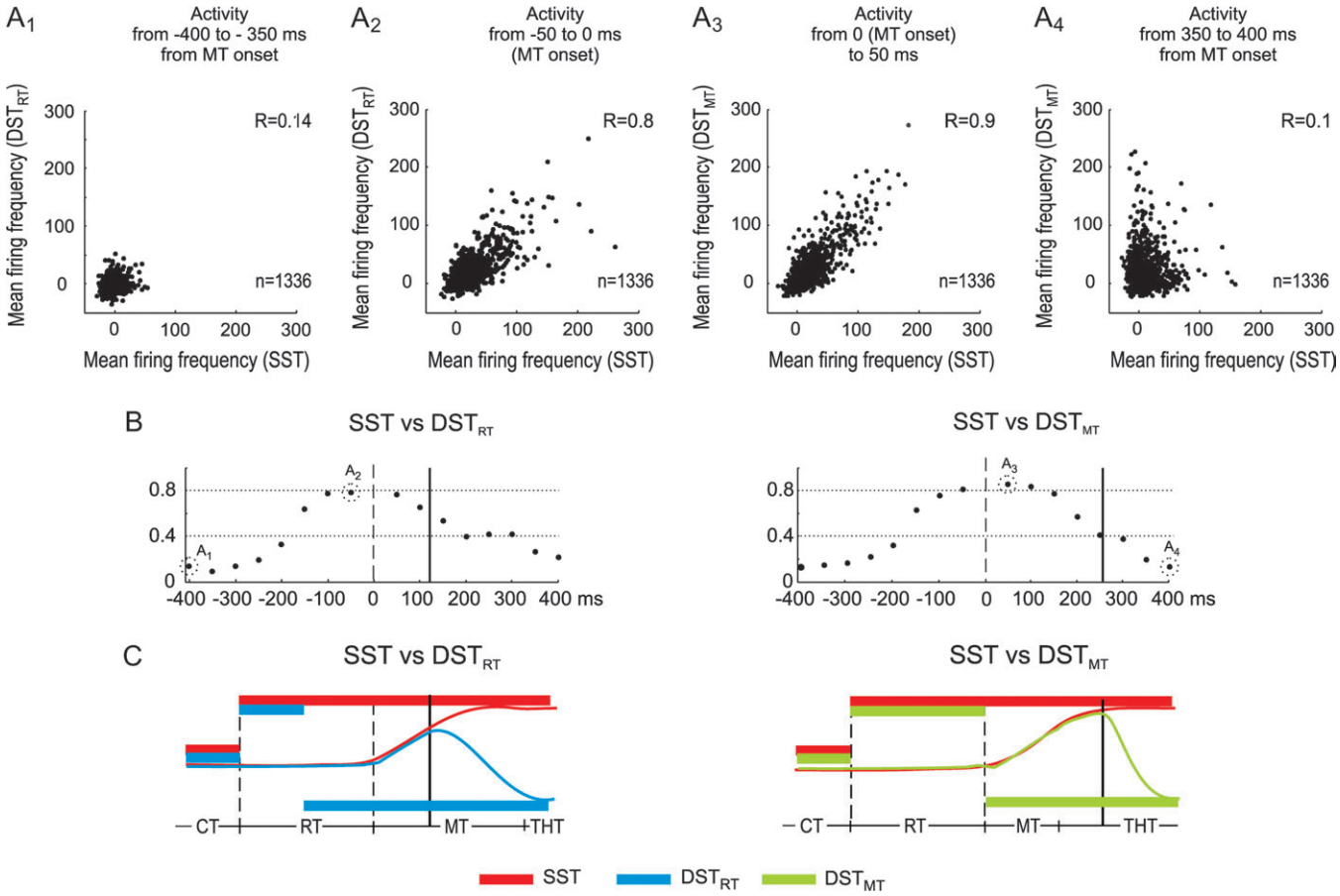

Figure 13. Comparison of cell activity in SST and DST conditions. (*A*) Examples of scatter plots of neural activity across task conditions (*A1-2*: SST vs. DST_{RT}; *A3-4*: SST vs. DST_{MT}) at different 50 ms time bins, where n indicates the number of comparisons performed (167 hand-related cells × 8 reach directions). (*B*) Evolution in time of the correlation coefficient (*R*), 400 ms before to 400 ms after hand MT onset (0 ms) for 2 different task comparisons. The circled values correspond to the R values obtained from the 4 scatter plots shown in (*A*). (*C*) Schematic representation of tasks and sequence of behavioral events. Left panel compares SST and DST_{RT}, right panel SST and DST_{MT}. Thick colored bars represent the relative timing of the central and peripheral targets in the different tasks (red: SST, blue: DST_{RT}, green: DST_{MT}). Curves represent the schematic temporal evolution of hand position (red: SST; blue: DST_{RT}; green: DST_{MT}). In (*B*) and (*C*) the vertical solid line indicate the mean time of shift of hand trajectory.

100 ms of RT. At that time, the target had already been switched for the DST_{RT}, and the animals were ready to move (orienting their hand toward the first target). The correlation in cell firing frequency started to decrease immediately after MT onset, approximately 150 ms after the presentation of the second target. A similar phenomenon could be observed in the

SST versus DST_{MT} comparison (Fig. 13*B*,*C*, right panels). Before the beginning of MT the correlation in firing frequencies attained its highest values after 150 ms from the first target onset. As in the previous case, this final part of RT preceded a hand movement that was initially directed toward the first target. Then, after MT onset, the correlation was maintained at ~0.8 and significantly decreased at 0.57 after 150 ms, that is, 150 ms following the presentation of the second target.

Overall, these observations suggest that the neural activity was scarcely influenced within the first 150 ms after target presentation, regardless of whether this target was the first or the second one, and regardless of whether the second target was presented during the RT or at the beginning of MT. A signal concerning the specification of future hand movement trajectory only emerged shortly after this time.

Divergence of Cell Activity between SST and DST Conditions

In Figure 14, the pop-SDFs were computed for different task conditions by using only hand-related cells from Monkey 1. The results obtained from Monkey 2 were virtually identical. In each panel, neural activity during the DST (thick gray line) is compared with that observed during the SST (thick black line). To this purpose, for single-step trials we have used the activity at the preferred direction, whereas for the double-step trials we have considered the activity observed when the first target was located in the cell's preferred direction and the second one in the opposite direction. In other words, for the DST we have considered the neural activity associated with hand movements that changed from the preferred to the antipreferred direction. These comparisons were performed when target jump occurred either during RT (Fig. 14*A*) or at the onset of MT (Fig. 14*B*).

In both instances the population activity sharply increased at about 120 ms from the first target presentation. This increase was initially similar in the SST and DST, and then in the latter the cell activity significantly diverged from that of the SST at a time that depended on the timing of the target jump in DST tasks. In the DST_{RT} task, the divergence occurred at about 140 ms following the second target presentation, almost in coincidence with the MT onset (Fig. 14*A*). A different value was obtained during the DST_{MT} (Fig. 14*B*). In this case the time of divergence of the 2 pop-SDFs occurred 216 ms after the second target was lit, that is, 216 ms after the hand started to move.

The divergence of the pop-SDFs always preceded the time of shift in hand trajectory (Fig. 14). When the target jumped

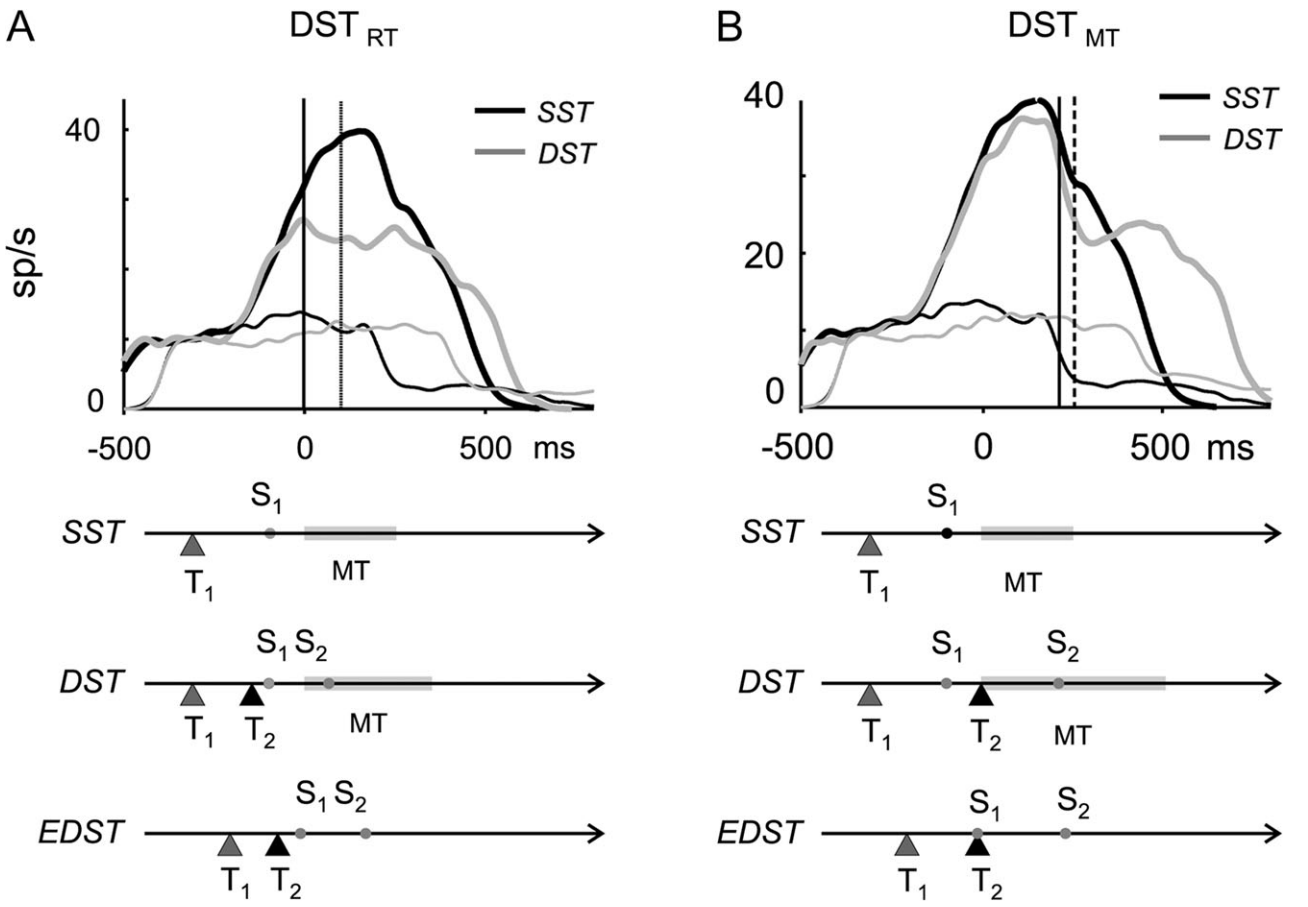

Figure 14. Population activity across task conditions. Population SDF (pop-SDF) are compared across the *Reaching* (thick curves) and *Saccade* (thin curves) tasks, in SST (black) and DST (gray), when the target jumped during RT (DST_{RT}; *A*) and when the sudden change occurred at the MT onset (DST_{MT}; *B*). Pop-SDF were obtained by combining single-cell activity of hand (or eye) movements made toward the preferred direction of each cell, then to the opposite one. The time scale is aligned to the onset of hand movement (0 ms). The vertical dashed lines indicate the moment of change of hand trajectory, the vertical solid line is the moment at which neural activity in DST significantly diverges from that of SST. The arrows below illustrate the temporal sequence of behavioral events. T_1 and T_2 indicate the mean time of presentation of the first and second target; S_1 and S_2 the mean onset of the saccade to the first and to the second target; MT indicates the mean duration of hand movement.

during the RT, the change in neural activity led the shift in hand trajectory by about 100 ms, whereas this difference tended to be shorter when the target jumped at the onset of MT.

In all instances, the population activities of these hand-related cells were very weak when studied during the Saccade task conditions (thin lines), as expected from the cell selection procedure adopted in this study (see Methods). This analysis confirms what has been described in the previous paragraph. In fact when the target jumped during the RT, during the first part of MT the activity of the DST is significantly different from that of the SST, contrary to the case of the DST with target switch at the onset of MT, when the population activities are very similar.

Discussion

Behavioral Performance

In this study the animals' hand movements unfolded in 3D space and were in all respects similar to natural movements. Movement trajectories were the results of training during which the animals freely selected their hand paths to the target. This fast hand movement was interrupted when the target suddenly jumped from its original position to a new one, either during RT or at the onset of MT. The in-flight correction necessary to bring the hand to the new target's position resulted in a curved trajectory. The intermingled design of the task did not allow the animals to predict whether they had to perform a single or a double-step movement. Under these conditions, no delays were observed, beyond the expected RT, for movements toward the second target. Instead, the RT to this target (RT_2) was significantly shorter than that to the first one, as well as to those observed in the SST. Furthermore the length of RT_2 tended to be shorter, when the time elapsing between the first and the second target increased. In humans performing free double-step movements as in our study, a reduction of the RT to the second target has also been described by different studies. In fact, it has been shown that the minimum delay for correcting a movement can be 200, or even 150 ms according to the level of predictability (Carlton 1981). Soechting and Lacquaniti (1983) have reported that on average, the RT to the change in target location was 90% that of the RT to the initial command signal. Finally, when the ISI is around 100 ms (van Sonderen et al. 1989), on average, double-step trajectories deviate from their original ones within 60 ms, with a shift time of 160 ms. The RT to a second target is also affected by a number of target features and it is characterized by significant intersubject variability (Veerman et al. 2008).

In our study, the observed shorter length of the RT to the second target (RT_2) relative to that to the first one can be tentatively explained by the phenomenon observed by Churchland et al. (2006) in premotor cortex. These authors have reported that longer RTs were associated with trials with more variable firing rate. In our case, the firing rate of each cell across trials with similar movement conditions was characterized by a higher variability of neural activity within the first part of the RT. When the firing rates of each cell in the single and DSTs at different time bins are compared, this "inconsistency" of rates was indicated by the low values of correlation coefficients in the initial part of the RT. In contrast, in the latest part of the RT and at the beginning of the MT, the higher values of the correlation coefficients might be regarded as resulting from a decrease in the variability of the cell's response across trials. Therefore, according to the hypothesis proposed by Churchland et al. (2006), the shorter RT after the second target presentation in our study is to be expected on the basis of the higher consistency of firing rates at that stage of task execution, with respect to the beginning of the trial, and so can be regarded as an expression of an advanced level of motor preparation. The same phenomenon might explain the observed tendency of the RT to decrease when the target jump approaches (or coincides with) the onset of MT. In fact, in this case RT_2 begins in a condition of an appropriate state of firing rate that would minimize the RT duration. This ideal state is expressed by the low variability across conditions.

Considering the findings overall, for actions that can be fluently blended one into the other, at least under the conditions of rapid changes of hand trajectory during free reaches to visual targets as opposed to making 2 distinct responses, these data do not support the existence of a psychological refractory period (Telford 1931; Welford 1952, 1959; see Bartelson 1966; Georgopoulos et al. 1981; Pashler and Johnston 1998, for discussion). It is believed that during the latter, determining how one should respond to a second stimulus, and thus making the motor response to it, is delayed in a central bottleneck, while the first stimulus is being processed.

Contrary to what is observed for hand movements, in the double-step paradigm saccades to the first target were never interrupted by the presentation of a second one. In spite of this, the higher velocity enabled the eye to attain the second target well before the hand. This dissociation between eye and hand motor behavior during reaching tasks has already been described (Georgopoulos et al. 1981).

Neural Control of Hand Trajectory

The main result of this study, as well as of previous ones on the same subject, is that motor commands for fast movements can be updated in a continuous and dynamic fashion by changing the visual information that guides movement. In terms of the encoding mechanism, the neural representation of online control might reside in the relationships of parietal cell activity with hand kinematics, as shown by the regression model used to fit neural activity, based on parameters such as hand position (Georgopoulos et al. 1984; Lacquaniti et al. 1995: Johnson et al. 1996), speed (Ashe and Georgopoulos 1994; Averbeck et al. 2005), and movement direction (Kalaska et al. 1983, 1990; Ashe and Georgopoulos 1994; Johnson et al. 1996; see Battaglia-Mayer et al. 2003 for a review). We believe that it is through the graded influences of the above signals on neural activity that the information about change of movement trajectory can be encoded. In many cells, the change of neural activity leads, and therefore predicts, the change of kinematics necessary to modify hand movement trajectory. For other cells, the change of neural activity follows that of hand trajectory, thus being influenced by movement execution signals thanks to feedback mechanisms originating from the moving limb. As a consequence of the strict relationships between parietal cell activity and hand kinematics, the activity associated with the DST can be predicted from what is observed during the single-step movement. In other words, in parietal cortex, the activity associated with a more complex arm movement can be to a certain extent "reconstructed" through the activity patterns typical of single segments of the entire movement, those into

which a given action can be decomposed. An epiphenomenon of this potential function of specifying future hand kinematics is the apparent interruption of the cell discharge observed for the movement toward the first target, and its substitution with a new one, similar to that observed for the movement to the second target.

Whether this substitution of discharge pattern is the result of the computation of a new motor command, rather than the updating of the old one cannot be decided on the basis of the present experiment. This operation seems computationally efficient, because it neither requires the emergence of a new relationship between neural activity and movement parameters, nor the encoding of a correction signal by a specialized subpopulation of parietal neurons, but only the graded utilization of kinematic variables, such as hand position, movement direction and velocity, all already combined at the single-cell level.

Time for the Visuo-motor Transformation

Another crucial question concerns when in the PPC the visual signal about target location, that determines the future movement trajectory, influences neural activity. The answer to this question emerged from the analysis of the temporal evolution of the correlation between the neural activity observed in the single-step and in the double-steps conditions, for movements oriented initially to the same target. In general, after visual target presentation, parietal neural activity does not seem to encode the future hand movement direction until 150 ms after the moment of target presentation. This was true whether the hand moved to the first or to the second target and whether the second target was presented in the middle of RT or at the beginning of MT. In each of these cases, the temporal evolution of the correlation in cell firing frequencies between SST and DST only started to change at 150 ms following the presentation of the first or second target. Therefore, this interval may be considered as the time necessary for the visuo-motor transformation underlying reaches to visual targets to occur. This value is reminiscent of that necessary for motor preparation after target onset reported by Churchland et al. (2006) in premotor cortex. Furthermore, the results obtained from our correlation analysis are in line with the optimal-subspace hypothesis (Churchland et al. 2006) according to which the brain actively tends to bring firing rates to a particular state, necessary to achieve the desired result at the motor output level. In our study, we confirm this hypothesis, even though from a different perspective. The emergence of an optimal state is indicated by the high correlation of firing rates across different movement conditions, in proximity of the hand movement onset. In other words, it is likely that during this phase of the task each cell reaches its own optimal firing state that is independent of the task demands (SST, DST_{RT}, DST_{MT}), thus leading to a high correlation when different conditions are compared.

Encoding of a New Trajectory during the Execution of Arm Movement

The results of this study are also relevant to the issue of the coexistence of neural signals concerning execution of hand movement along a given trajectory, and ones involved in the planning of a different one. Under specific circumstances, these 2 aspects of behavior seem to be simultaneously encoded by neural activity.

We propose that the hand RT to visual targets is divided into 2 components; the first has a fixed duration of approximately 150 ms that would correspond to the time necessary for the visuo-motor transformation, whereas the second of variable duration would correspond to the trajectory specification. Coexistence of signals about ongoing movement with those concerning planning a different one occurs only when the second portion of RT_2, that is, the time beyond 150 ms after second target onset, overlaps with the hand movement to the first target (Fig. 15).

The observation supporting this statement is that the correlation in firing frequencies between SST and DST_{RT} dropped-off at the onset of hand movement (Fig. 13*B*), even though the hand trajectories in both conditions were still identical (Fig. 13*C*). This decrease in correlation might be due to the emerging influence of the planning of a new trajectory on the execution of the current one. Noticeably, when comparing the firing frequencies in SST and DST_{MT}, the correlation remained high during the first part of MT and decreased only 150 ms after the initiation of hand movement (Fig. 13).

Therefore, for this coexistence to be detected, the presentation of the second target should occur in a time period around the MT onset. This period must be such that the final part of the RT_2 (carrying information about the new direction) overlaps the MT (Fig. 15). This implies that the target jump should occur not too early relative to the first target presentation and not too late relative to the target onset, otherwise the 2 signals cannot coexist.

The coexistence of predictive and movement execution signals is also suggested by the temporal evolution of the population responses in the SST and DST, and by the specific time these 2 responses diverged from each other. When the second target was presented during the RT, the divergence occurred at about 100 ms before the change of direction of hand movement. Therefore, in the interval between the divergence in neural activity and the shift in hand movement a new signal related to the preparation of a future change in hand trajectory emerged. However, when the target jump occurred at the onset of the hand movement, the divergence of

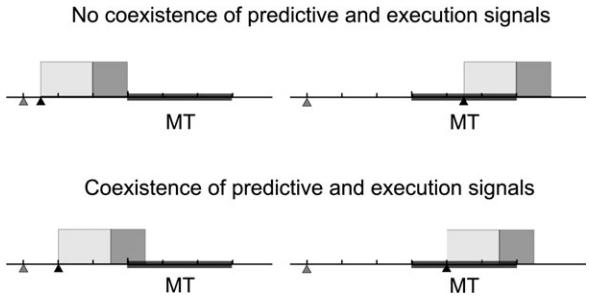

Figure 15. Schematic representation of temporal events (duration of RT and MT) representing examples of the conditions for coexistence (or no coexistence) of predictive signals with those related to hand movement execution. The triangles refer to the appearance of the visual targets, the black bar to the duration of MT and the gray (light and dark) rectangle represents the duration of RT_2. The light gray area refers to the first part of RT_2 (lasting 150 ms) not influenced by the future hand movement direction, whereas the dark gray one represents the last part of RT encoding update of hand movement trajectory. Only in those conditions where the dark gray portion overlaps the MT (black bar), the 2 signals coexist.

the population activity was detected nearer (about 50 ms before) to the change in the hand kinematics. We attribute these results to the different lengths of the RTs to the second target for the different times at which the target jumps. In fact, assuming that during the first 150 ms of RT, the neural activity is not influenced by the direction of the future arm movement, only the last 120–130 ms should be the period in the DST_{RT} (where RT_2 lasts about 270–280 ms) where a signal due to the preparation of a response in a new direction emerges. Accordingly in the DST_{MT}, where RT_2 tends to be shorter, this period should be expected to be shorter too, as it is.

In addition, the coexistence of predictive signals with those related to the movement kinematics is also suggested by the difference in the results of the multiple-linear regression, which takes into account only the kinematics parameters, when it was applied separately to the SST and DST conditions. The better performance of the regression analysis in the SST rather than in the DST might be explained by the presence, in the latter, of a signal related to the preparation of a new trajectory, in addition to that related to the current one.

The Parieto-Frontal Network

This study can be interpreted within the framework of the visuo-motor operations performed by the parieto-frontal system. The region of area 5 where cell activity has been studied, that is, area PE, is linked to motor cortex both directly (Strick and Kim 1978; Johnson et al. 1996; Matelli et al. 1998; Marconi et al. 2001), and indirectly, via the dorsal premotor cortex (Johnson et al. 1996; Matelli et al. 1998), which in turn projects to motor cortex (see Muakkassa and Strick 1979; Johnson et al. 1996). Therefore, it is not surprising that certain of the results of this study, on one side resemble those obtained in motor cortex by the only other cell recording study available in the literature (Georgopoulos et al. 1983) on online control of hand movement. On the other side, though from another perspective related to the issue of the time necessary for motor preparation, they are also consistent with the observations done in premotor cortex (Churchland et al. 2006).

A Positive Image of the Motor Disorders of the Parietal Syndrome

A common disorder that follows a lesion in the PPC is optic ataxia (OA), which is characterized by defective visual control of arm reaching, accompanied by defective hand orientation and grip formation. A case report of a patient with a large bilateral parietooccipital lesion, and which is therefore problematic for an interpretation in terms of the exact anatomical location of the site responsible of the deficits, stresses 2 main features (Pisella et al. 2000; Grea et al. 2002) of OA (for a recent review, see Battaglia-Mayer and Caminiti 2002; Battaglia-Mayer et al. 2006) that are of interest to the results of the present study. The first is the defective control of the directional components of hand movement, including a marked failure to make smooth corrective adjustments after a target jump. The second is the claim that OA derives from an impairment of automatic control, rather than movement planning per se. In this OA patient, the hand movement to a visual target cannot be updated after a sudden target jump, but is fully completed to the first target's position, before the hand changes its direction and moves toward the new target's location.

The failure of such an OA patient to make fast, in-flight corrections of the hand movement trajectory may be dependent on the loss of those populations of parietal cells whose activity carries signals concerning corrections of hand movement direction, prompted by a change of the visual sensory information that dictates the new movement end-point. Therefore, the results of our study provides a "positive image" of some crucial signs of OA in parietal patients, also suggesting that in humans the observed impairment can be due to lesion of the SPL. If PPC cells are responsible for the future direction of movement and also the change of movement trajectory depends on inputs to PPC cells smoothly altering their relative firing rates, then loosing these predictive cell populations will impair both reaching and trajectory modification. Therefore, the inability to adjust trajectory should not be the basic problem of parietal patients suffering from OA.

Supplementary Material

Supplementary material can be found at: http://www.cercor.oxfordjournals.org/

Funding

Ministry of University and Scientific Research of Italy; Canadian Institutes of Health Research and Ministry of University and Scientific Research of Italy supported P.S.A.

Notes

We are very grateful to Professor Tim Shallice for his critical review of the manuscript. *Conflict of Interest*: None declared.

Address correspondence to Professor Alexandra Battaglia-Mayer, Dipartimento di Fisiologia umana e Farmacologia, SAPIENZA Università di Roma, Piazzale Aldo Moro 5, 00185 Rome, Italy. Email: alexandra.battagliamayer@uniroma1.it.

References

Andersen RA, Buneo CA. 2002. Intentional maps in posterior parietal cortex. Annu Rev Neurosci. 25:189–220.

Ashe J, Georgopoulos AP. 1994. Movement parameters and neural activity in motor cortex and area 5. Cereb Cortex. 6:590–600.

Averbeck B, Chafee M, Crowe D, Georgopoulos AP. 2005. Parietal representation of hand velocity in a copy task. J Neurophysiol. 93:508–518.

Bard C, Turrell Y, Fleury M, Teasdale N, Lamarre Y, Martin O. 1999. Deafferentation and pointing with visual double-step perturbations. Exp Brain Res. 125:410–416.

Bartelson P. 1966. Central intermittency twenty years later. Q J Exp Psychol. 18:153–163.

Battaglia-Mayer A, Caminiti R. 2002. Optic ataxia as a result of the breakdown of the global tuning fields of parietal neurones. Brain. 125:225–237.

Battaglia-Mayer A, Archambault PS, Caminiti R. 2006. The cortical network for eye-hand coordination and its relevance to understanding motor disorders of parietal patients. Neuropsychologia. 44:2607–2620.

Battaglia-Mayer A, Caminiti R, Lacquaniti F, Zago M. 2003. Multiple levels of representation of reaching in the parieto-frontal network. Cereb Cortex. 13:1009–1022.

Battaglia-Mayer A, Ferraina S, Mitsuda T, Marconi B, Genovesio A, Onorati P, Lacquaniti F, Caminiti R. 2000. Early coding of reaching in the parietooccipital cortex. J Neurophysiol. 83:2374–2391.

Battaglia-Mayer A, Ferraina S, Genovesio A, Marconi B, Squatrito S, Molinari M, Lacquaniti F, Caminiti R. 2001. Eye-hand coordination

during reaching. II. An analysis of the relationships between visuomanual signals in parietal cortex and parieto-frontal association projections. Cereb Cortex. 11:528–544.
Blouin J, Teasdale N, Bard C, Fleury M. 1995. Control of rapid arm movements when target position is altered during saccadic suppression. J Mot Behav. 27:114–122.
Carlton LG. 1981. Processing visual feedback information for movement control. J Exp Psychol Hum Percept Perform. 7:1019–1030.
Churchland MM, Byron MY, Ryu SI, Santhanam G, Shenoy KV. 2006. Neural variability in premotor cortex provides a signature of motor preparation. J Neurosci. 26:3697–3712.
Della-Maggiore V, Malfait N, Ostry DJ, Paus T. 2004. Stimulation of the posterior parietal cortex interferes with arm trajectory adjustments during the learning of new dynamics. J Neurosci. 24:9971–9976.
Desmurget M, Epstein CM, Turner RS, Prablanc C, Alexander GE, Grafton ST. 1999. Role of the posterior parietal cortex in updating reaching movements to a visual target. Nat Neurosci. 2:563–567.
Desmurget M, Grafton S. 2000. Forward modeling allows feedback control for fast reaching movements. Trends Cogn Neurosci. 411:423–431.
Georgopoulos AP, Kalaska JF, Massey JT. 1981. Spatial trajectories and reaction times of aimed movements: effects of practice, uncertainty, and change in target location. J Neurophysiol. 46:725–743.
Georgopoulos AP, Kalaska JF, Caminiti R, Massey JT. 1983. Interruption of motor cortical discharge subserving aimed arm movements. Exp Brain Res. 49:327–340.
Georgopoulos AP, Caminiti R, Kalaska JF. 1984. Static spatial effects in motor cortex and area 5: Quantitative relations in a two-dimensional space. Exp Brain Res. 54:446–454.
Grea H, Pisella L, Rossetti Y, Desmurget M, Tilikete C, Grafton S, Prablanc C, Vighetto A. 2002. A lesion of the posterior parietal cortex disrupts on-line adjustments during aiming movements. Neuropsychologia. 40:2471–2480.
Johnson H, Haggard P. 2005. Motor awareness without perceptual awareness. Neuropsychologia. 43:227–237.
Johnson PB, Ferraina S, Bianchi L, Caminiti R. 1996. Cortical networks for visual reaching: physiological and anatomical organization of frontal and parietal lobe arm regions. Cereb Cortex. 6:102–119.
Kalaska JF, Caminiti R, Georgopoulos AP. 1983. Cortical mechanisms related to direction of two dimensional arm movements: relations in parietal area 5 and comparison with motor cortex. Exp Brain Res. 51:247–260.
Kalaska JF, Cohen DAD, Prud'Homme M, Hyde ML. 1990. Parietal area 5 neuronal activity encodes movement kinematics, not movement dynamics. Exp Brain Res. 80:351–364.
Lacquaniti F, Guigon E, Bianchi L, Johnson PB, Ferraina S, Caminiti R. 1995. Representing spatial information for limb movement: the role of area 5 in the monkey. Cereb Cortex. 5(391):409.
Lee J-H, van Donkelaar P. 2006. The human dorsal premotor cortex generates on-line error corrections during sensorimotor adaptation. J Neurosci. 26:3330–3334.
Marconi B, Genovesio A, Battaglia-Mayer A, Ferraina S, Squatrito S, Molinari M, Lacquaniti F, Caminiti R. 2001. Eye-hand coordination during reaching. I. Anatomical relationships between parietal and frontal cortex. Cereb Cortex. 11:513–527.
Matelli M, Govoni P, Galletti C, Kutz DF, Luppino G. 1998. Superior area 6 afferents from the superior parietal lobule in the macaque monkey. J Comp Neurol. 402:327–352.
Moran DW, Schwartz AB. 1999. Motor cortical representation of speed and direction during reaching. J Neurophysiol. 82:2676–2692.
Muakkassa KF, Strick PL. 1979. Frontal lobe inputs to primate motor cortex: evidence for four somatotopically organized "premotor" areas. Brain Res. 177:176–182.
Pashler H, Johnston JC. 1998. Attentional limitations in dual-task performance. In: Pashler H, editor. Attention. Hove, UK: Psychology Press/Erlbaum and Taylor & Francis. p. 155–189.
Pelisson D, Prablanc C, Goodale MA, Jeannerod M. 1986. Visual control of reaching movements without vision of the limb. II. Evidence of fast unconscious processes correcting the trajectory of the hand to the final position of a double-step stimulus. Exp Brain Res. 62:303–311.
Pisella L, Grea H, Tilikete C, Vighetto A, Desmurget M, Rode G, Boisson D, Rossetti Y. 2000. An 'automatic pilot' for the hand in human posterior parietal cortex: toward reinterpreting optic ataxia. Nat Neurosci. 3:729–736.
Raghunathan TE, Rosenthal R, Rubin DB. 1996. Comparing correlated but nonoverlapping correlations. Psychol Methods. 1:178–183.
Sarlegna FR, Gauthier GM, Bourdin C, Vercher JL, Blouin J. 2006. Internally driven control of reaching movements: a study on a proprioceptively deafferented subject. Brain Res Bull. 69:404–415.
Soderkvist I, Wedin P-A. 1993. Determining the movements of the skeleton using well-configured markers. J Biomech. 26:1473–1477.
Soechting JF, Lacquaniti F. 1983. Modification of trajectory of a pointing movement in response to a change in target location. J Neurophysiol. 49:548–564.
Strick PL, Kim CC. 1978. Input to primate motor cortex from posterior parietal cortex (area 5). I. Demonstration by retrograde transport. Brain Res. 157:325–330.
Telford CW. 1931. The refractory phase of voluntary and associative responses. J Exp Psychol. 14:1–36.
van Sonderen JF, Gielen CCAM, van der Gon Denier JJ. 1989. Motor programmes for goal-directed movements are continuously adjusted according to changes in target location. Exp Brain Res. 78:139–146.
Veerman M, Brenner E, Smeets J. 2008. The latency for correcting a movement depends on the visual attribute that defines the target. Exp Brain Res. 187:219–228.
Welford AT. 1952. The "psychological refractory period" and the timing of high speed performance. A review and theory. Br J Psychol. 43:2–19.
Welford AT. 1959. Evidence for a single channel decision mechanism limiting performance in a serial reaction-time task. Q J Exp Psychol. 11:193–210.